Joint Special Interest Group meeting between euspen and ASPE
Advancing Precision in Additive Manufacturing
Inspire AG, St. Gallen, Switzerland 2021
www.euspen.eu

Comparison of dimensional measurements from images acquired by synchrotron tomography with VGSTUDIO MAX and ImageJ

C. Cayron[1], A. De Soete[1], Y. Gaillard[2], C. Yardin[1], N. Coutant[3], R. Nanjareddy[3], P. Bouvet[2], A.-F. Obaton[1]

[1]*Laboratoire Commun de Métrologie (LCM), Laboratoire National de Métrologie et d'Essais (LNE), 75015 Paris, France*

[2]*Centre Technique des Industries de la Fonderie (CTIF), 92318 Sèvres, France*

[3]*Volume Graphics (VG) GmbH, 69115 Heidelberg, Germany*

charles.cayron@lne.fr

Abstract

Initiated by a working group of the French Confederation for non-destructive testing (NDT) (COFREND), a comparison using an artefact produced by an FA process was conducted between different laboratories. The artefact contained several type of defect inherent to the building process and was scanned by synchrotron radiation.
In this study, the tomographic images of two defects (spherical and cylinder) were analyses with two software: an open source software, ImageJ, (used by CTIF and LNE) and a commercial software, VGSTUDIO MAX (used by VG). For ImageJ software, we have determined the influence of the operator effect in the reproducibility of the measurement for each kind of defect and all size (from 0.3mm to 0.8mm). It appears that operators have a significant part in the reproducibility of the measurement by ImageJ. However, the values of spherical volume and cylinder area obtained by ImageJ are consistent with the values of VGSTUDIO MAX. Unfortunately, the real value of defect (spheres and Cylinders) are unknown.

Control, Dimensional, Image

1. Introduction

Thanks to the numerous developments that have been made over the years, additive manufacturing (AM), or 3D printing, currently appears to be the most relevant industrial solution to optimize the production of complex parts, almost impossible to implement by standard manufacturing processes [1]. However, the processes used in AM are still not fully mastered and a significant number of defects, inherent to the manufacturing method, can appear in the parts produced. The laser powder-bed fusion (L-PBF) process is one of the most used process for the manufacturing of metallic parts, especially for the aeronautic or medical fields. In this process, the defects occurring in the parts are layer defects, cross layer defects and the presence of unfused trapped powder [2]. X-ray computed tomography (XCT) is currently the most efficient method to characterize parts produced by additive manufacturing (AM) for its potential to inspect deep internal cavities in complex parts but also internal defects as well as to identify the different types of defects inherent to the used AM processes [3]. To characterize these type of defects, the most widely and efficient method used today is X-ray computed tomography (X-CT), which produces 2D X-ray images of an object from several angles to create a 3D data image by reconstruction. Then to analyse the integrity and perform dimensional measurements of the characterized objects from the images, a specific processing software needs to be used. The objective of this study is to observe the influence of this analysis software on the characterization of defects, resulting from the L-PBF process, between the commercial software VGSTUDIO MAX and the free software ImageJ. Within the ImageJ software, the study also wanted to determine if the operator processing the data had a significant influence on the value of the measured defect. This article will present first the experimental methodology of the study, then the data processing and finally the comparison between both software for each kind of defect.

2. Experimental protocol

2.1. Standard and software descriptions

Designed within the ISO/TC261-ASTM/F42 AM standardization joint group 59 "NDT for AM parts" and carried out by the French (LNE) and American (NIST) national metrology laboratories, the artefact used, called "Star Artefact", was produced in chrome-cobalt by the L-PBF process (**Figure *1***). This artefact contained several defects representative of the process and in particular two types of defects that will be studied in this paper: trapped powder in spheres and vertical cylinders (**Figure *2***). The size of the diameters of the spheres and cylinders varies between 0.2 mm and 0.8 mm. The "star artefact" was scanned with synchrotron radiation at the European Synchrotron Radiation Facility (ESRF) based in Grenoble (France) [4]. In this study, we used two different softwares to analyse spherical and cylinders defect presents in the Star Artefact. The first one is ImageJ, an open source image-processing program designed for scientific multidimensional images. The other software, VGSTUDIO MAX, is a high-end software for analyse and visualisation of computed-tomography data. First, to allow the measurement with ImageJ in the correct coordinate system (as ImageJ was not able to align the volume data from Synchroton), it was necessary to align it previously with VGSTUDIO MAX.

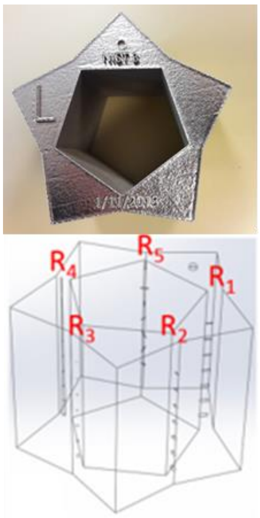

Figure 1. Picture (top) and schematic (bottom) of the star artefact

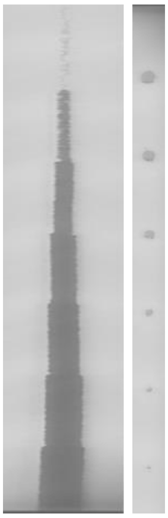

Figure 2. Images of vertical connected cylinders and spheres present in the star artefact

2.2. Measurement protocol for the spheres

ImageJ approach:

The measurement of the volume of the spheres (in number of voxel) is done in several steps determined by the operator. The measurement of the volume of each sphere is realised by calculating the area of the sphere on each 2D image and then summing them over all 2D images (77 2D images in our case). For the step one, the operator selects the sphere to measure and extracts the image volume from the original file. In the step 2, we inverse the colours on each image to determine the area of the sphere. (**Figure *3***). Then, the operators determines (step 4) the threshold on the lightest shade of grey to optimize the best area (**Figure *4***). As we can see, the threshold is determined according to the appreciation of each operator, which can affect the value of the measurement. Finally, the exercise being carried out according to the aspect of the sphere on a single view (according to x, y or z), rotations of 90° are performed on the image of the sphere to calculate the volume according to the other axes. Thus, for each sphere, the volume is calculated according to an average value on three different view of the sphere: front view, top view and left view.

The operator repeats all the operations three times in order to determine also the reproducibility of the process.

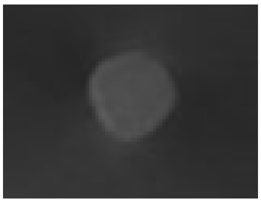

Figure 3. Spherical view after colour inversion

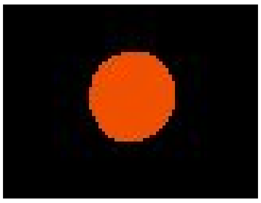

Figure 4. Spherical view after threshold determination

VGSTUDIO MAX approach: (released version 3.4.5)

The defect analysis procedure consists of two steps:

a) Each voxel is checked whether it is part of a defect. Groups of connected defect candidates are created.

b) Each group of defect candidates is checked whether it matches the parameters specified by the user. This algorithm identifies voxels as defects based on the actual local grey value of the material in relation to a specified local contrast threshold and can detect defects that are connected to the surrounding air. Finally, the borders of each defect candidate are locally adapted to the greatest grey value gradient. This approach calculates certain defect properties with *subvoxel* accuracy.

2.3. Measurement protocol for the cylinder

ImageJ approach:

For vertical cylinders characterization, a part of the cylinder was sliced in 119 images and we calculated the area for each slice. To facilitate the operations, an algorithm specific to ImageJ has been set up to take over the systematic operations that do not require a decision from the operator (cylinder positioning, size of the surface, extraction window, etc.). The first step is to, from the image of the aligned cylinders (**Figure *2***), position the extraction rectangle to select the area of the cylinder that he wishes to characterize (first contribution in operator effect). The algorithm defines rectangle's width in order to have the same number of measurements per operator. Next, the algorithm performs the operations of rotation (in order to see the cylinder from the front), binarize the image in black and white (**Figure *5***) and offers to the operator a list of filters (**Figure *6***) that he can use to calculate the area of each cylinder stack of 2D images. Therefore, in step 2, the operator chooses three different filters to apply on the cylinder surface images (second contribution in operator effect). Thus for each cylinder, 119 slices are made and the area is calculated (in number of pixels) for each slice according to three filters. For this part of the study, eight operators participated for measurements. Moreover, to facilitate the analysis of the results, the areas are measured in number of pixels (whose edge measures 23.52 µm).

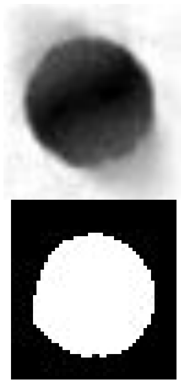

Figure 5. Example of image of the slice of the cylinder before and after applying a filter (here Default filter)

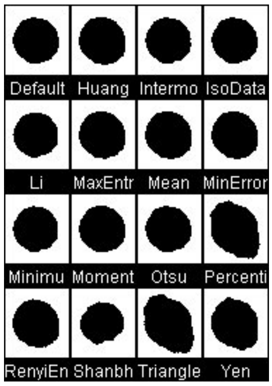

Figure 6. Proposal filters for area determination

VGSTUDIO MAX approach: (released version 3.4.5)

Surface determination including removing of noise particles and scanning artifacts was performed using the Advanced (classic) approach of VGTSTUDIO MAX, leading to a locally adaptive, subvoxel precise surface. This minimizes variance caused by operator influence. The star artefact was then aligned, and 48 regularly spaced Gauss circles were adjusted to the surface for each theoretical diameter. The area was then calculated using the mean diameter of the circles for each theoretical diameter.

3. Data processing

First, we checked the relevance of the data provided by the operators: standard statistical tests were conducted to test the dispersions of the values (Cochran test), the variance of the means (Fisher test) and the study of extreme values (Grubbs test). These tests allowed us to validate the consistency of the measurements made by the different operators, but also to identify the presence of outliers in the data sets of the different operators. The outliers were then extracted from the data so as not to disturb the variance and mean calculations. In the case of the spheres, 16 values were removed out of a total of 756 values. In the case of cylinders, 4 values out of 48 measurements were not retained.

Nevertheless, the operator remains the main actor in the measurement chain and his different actions can influence the measurement result. One of the questions of this study was therefore to determine and quantify, if necessary, the impact of the operator on the measurement using ImageJ. Indeed, in the case of the measurement of the volume of a sphere, the operator can influence the measurement during the last processing step, when he performs the thresholding step to define the grey area to calculate. The operator defines the level of threshold he wants apply on the stack of images which will defines the final volume of the sphere.

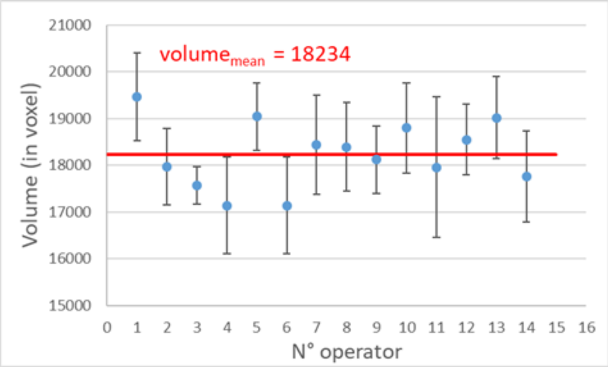

Figure 7 : volume measured by each operator for spherical of 0.8 mm

Figure 7 shows the result of the volume measurements for each operator in the case of the 0.8 mm sphere. The values presented by operator are the average values over the 3 measurements that were made on all the views (for recall top, front and left view). All the measurements show volume values in a range from 17000 voxels to 20000 voxels. From these measurements, we determined the influence of the operator from the following equation:

$$\sigma_{op}^2 = \sigma_R^2 - \sigma_r^2 \qquad (1)$$

where σ_r and σ_R are the standard deviation of repeatability and reproducibility, respectively.

The reproducibility of the measurements is determined from the calculation of the variance over all the measurements of all the operators, while the repeatability is calculated from the standard deviations of each operator by the relation:

$$\sigma_r = \sqrt{\frac{\sum_i \sigma_i^2}{N}} \qquad (2)$$

where N is the number of operator and i =1,..., N

4. Results

For all the measured spheres, we were able to determine the influence of the operator on the measurement error. Table 1 summarizes all the results for spheres from 0.3 mm to 0.8 mm.

We can see from Table 1 that the smaller the theoretical volume of the sphere to be measured, the greater the error in the measurement. Similarly, the impact of the operator on the value of the measured volume is also more important when the size of the sphere is decreasing. Indeed, the smaller the volume of the sphere is, the less the sphere slice contains pixels. Thus, when the operator defines his thresholding level, a small variation of this level will affect more the small volumes than the large volumes. Moreover, due to its manufacturing process, the 0.3 mm sphere is less defined than the 0.8 mm sphere that also affects the quality of the measurement.

Table 1: Results of spherical volumes and operator effect by ImageJ

Theoretical diameter	Measured volume (voxel)	σ_r	σ_R	Operator effect
0.8 mm	18234	939	1122	613
0.7 mm	11696	656	844	532
0.6 mm	7038	547	648	348
0.5 mm	3245	250	342	233
0.4 mm	1208	128	196	148
0.3 mm	353	99	151	114

From these results, we compared the volume measurements made by ImageJ with those made by the VGSTUDIO MAX software that provides 3D volume defect in subvoxel accuracy.

Table 2: Spherical volumes comparison for ImageJ and VGSTUDIO MAX

ImageJ		VGSTUDIO MAX	Relative difference (%)
Measured volume (voxel)	σ_R	Measured volume (voxel)	
18234	1122	18512	-1.50%
11696	844	11895	-1.67%
7038	648	7216	-2.46%
3245	342	3508	-7.51%
1208	196	1319	-8.39%
353	151	331	6.52%

Table 2 shows the results of the sphere volume measurements according to the two software. First, we can see that the values obtained are consistent with each other: the values obtained by VGSTUDIO MAX are always within the standard deviations related to the reproducibility of the measurement by ImageJ. Moreover, we can also note that the larger the sphere, the smaller the relative difference between the measurements of the two software. Indeed, the larger the sphere is, the less the error on the contour of the sphere will have consequences on the result. Finally, it seems that, with the exception of the 0.3 mm sphere, the ImageJ software always overestimates the volume of the sphere compared to the VGSTUDIO MAX software. In the case of the 0.3 mm sphere, this different behaviour may come from the difficulty to measure precisely its volume: the reproducibility of the measurement by ImageJ is equivalent to half the value of its volume.

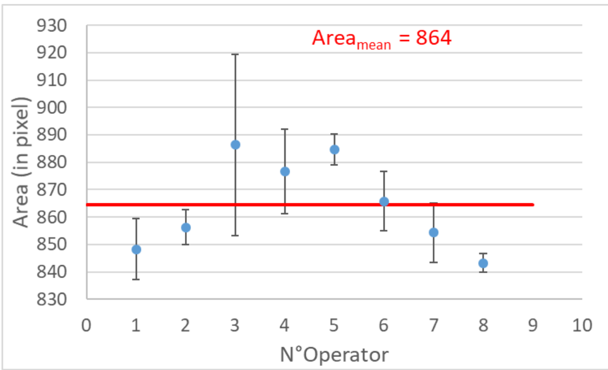

Figure 8 : Surface measured by each operator for cylinder of 0.8 mm

Figure 8 shows the result of the average value of the areas calculated using the set of filters chosen by each operator for the cylinder of 0.8 mm. The set of measurements shows a mean value of 864 pixels for a data dispersion between 840 pixels and 890 pixels. First analysis on the average shows that operator effect is not on the average value of the area but in the dispersion of values between operator. This dispersion is principally due to the filter used to determinate the area. In fact, we can see that operator 3 has a much larger dispersion between its used filters than operator 8.

This difference can be explained by the difference in filters used: operator 3 used the Minimum, Li, Default filters while operator 8 chose the Default, Mean, Otsu filters. Indeed, each filter has its own convolution method to define the area to be measured, which can therefore give different values: it seems that the combination of some filters, such as Default, Mean, Otsu or Huang, shows very close values of areas while the combination of other filters Li, Minimum and Default gives more dispersive values.

Then for this cylinder (as for all the cylinder), we have applied the Cochran test and it appeared that the operator 3 has an aberrant value of dispersion that should not be consider for the operator effect analyse.

Table 3: Mean area of cylinder slice and operator effect with ImageJ

Theoritical diameter	Area (pixel)	Repetability σ_r (pixel)	Reproductibility σ_R (pixel)	Operator effect (pixel)
0.8 mm	864	17	17	0
0.7 mm	631	19	19	0
0.6 mm	436	11	19	16
0.5 mm	289	8	13	15
0.4 mm	165	6	6	0
0.3 mm	76	8	8	0

Table 3 summarizes all the area values obtained for each cylinder diameter with the values of repeatability, reproducibility and the operator effect. It is noticeable that for four cylinder on six, there is no operator effect (repeatability and reproducibility being equal). This can be explain by the choice of the filter made by each operator: for both cylinder that have an operator effect, operators used principally filter that gave a bigger dispersion of value. Then, for cylinder that has not operator effect, the repeatability take count of the filter influence.

Table 4: Cylinders areas comparison for ImageJ and VGSTUDIO MAX

Theoritical diameter	ImageJ		VGSTUDIO MAX		Relative difference (%)
	Area (pixel)	σ_R (pixel)	Area (pixel)	σ_r (Pixel)	
0,8 mm	864	17	854	1,7	1,2%
0,7 mm	631	19	623	1	1,3%
0,6 mm	436	19	418	1,2	4,2%
0,5 mm	289	13	280	1,2	3,2%
0,4 mm	165	6	160	1,2	3,0%
0,3 mm	76	8	69	1,2	10,5%

Table 4 shows the results of the measurements of the average area of the cylinder slices by the analysis of both software: ImageJ and VGSTUDIO MAX. The repeatability σ_r of VGSTUDIO MAX values are calculated on the 48 Gauss cercles.

The results obtained are consistent with each other: the reproducibility errors of ImageJ values overlap the VGSTUDIO MAX values. As in the case of sphere volume measurements, the areas calculated by ImageJ are systematically greater than those obtained by VGSTUDIO MAX. The Gaussian approach used in this case should better define the boundaries compared to the one used by ImageJ which is a convolution method of the pixel colors with respect to the neighbours.

5. Conclusions and discussion

In this study, we have seen that in the case of spheres measurements, the operator effect is the main component of the reproducibility. For cylinder measurement, it appears that the choice of the filter is the principal contributor to the reproducibility. We also compared the values obtained by the two software and found that the values obtained were comparable, even if the values obtained by ImageJ are generally higher than those obtained by VGSTUDIO MAX.

To go further in this analysis, it would be interesting, within the framework of the measurement of the cylinders, to better determine the influence of the choice of the filter independently of the selected region. Two possibilities could be envisaged: the first one is to increase the size of the selected region to include nearly all the cylinder (if possible). The second possibility is to study the whole of the filters in order to determine, for the same selected region, all the differences related to them, then to perform once again the comparison of the operators by fixing in the protocol the filters.

Finally, it should be noted that the comparison between these software was not carried out under the best conditions: the data obtained by VGSTUDIO MAX were diameters (in mm) for cylinders while those of ImageJ were surfaces or volumes in number of pixel (respectively voxel). It would therefore be relevant to make a new comparison without having to convert a type of data from one software to another. It would be necessary, after we determine all the influent parameters of the operator effect for ImageJ, to do the same study on a case where real values are known.

Aknowledgement

Authors would like to thanks all the operators of this study and specifically L-F. Lafon, L. Fournet-Fayard, A. Choubib, S-C. Togue-tagne, S. El Ghazouali, Y. Longa, A. Mouillet, I. Mouslime, G. Le Breton, L. Diez-Jahier.

This work has been investigated in the frame of a XCT group of the French Confederation for non-destructive testing (COFREND) leads by L. Gay.

References

[1] W. Tao, M. C. Leu, “Design of lattice structure for additive manufacturing,” Proceedings of ISFA2016, 2016 International Symposium on Flexible Automation, Cleveland, Ohio, U.S.A., 1 - 3 August, 2016

[2] A-F. Obaton, B. Butsch, S. McDonough, E. Carcreff, N. Laroche, Y. Gaillard, J. Tarr, P. Bouvet, R. Cruz, A. Donmez, “Evaluation of Nondestructive Volumetric Testing Methods for Additively Manufactured Parts. In Structural Integrity of Additive Manufactured Parts”, N. Shamsaei, S. Daniewicz, N. Hrabe, S. Beretta, J. Waller, and M. Seifi: West Conshohocken, PA, pp 51–91, 2020, https://doi.org/10.1520/

[3] B. Dutton, W. Vesga, J. Waller, S. James, and M. Seifi, “Metal Additive Manufacturing Defect Formation and Nondestructive Evaluation Detectability,” in Structural Integrity of Additive Manufactured Parts, ed. N. Shamsaei, S. Daniewicz, N. Hrabe, S. Beretta, J. Waller, and M. Seifi (West Conshohocken, PA: ASTM International, 2020), 1–50. https://doi.org/10.1520/STP162020180136

[4] A. du Plessis, I. Yadroitsev, I. Yadroitsava, and S. G. Le Roux, ‘X-Ray Microcomputed Tomography in Additive Manufacturing: A Review of the Current Technology and Applications’, 3D Print. Addit. Manuf., vol. 5, no. 3, pp. 227–247, Jul. 2018, doi: 10.1089/3dp.2018.0060